Proceedings of EQUADIFF 2017
pp. 305–314

AN EFFICIENT LINEAR NUMERICAL SCHEME FOR THE STEFAN PROBLEM, THE POROUS MEDIUM EQUATION AND NONLINEAR CROSS-DIFFUSION SYSTEMS

MOTLATSI MOLATI* AND HIDEKI MURAKAWA†

Abstract. This paper deals with nonlinear diffusion problems which include the Stefan problem, the porous medium equation and cross-diffusion systems. We provide a linear scheme for these nonlinear diffusion problems. The proposed numerical scheme has many advantages. Namely, the implementation is very easy and the ensuing linear algebraic systems are symmetric, which show low computational cost. Moreover, this scheme has the accuracy comparable to that of the well-studied nonlinear schemes and make it possible to realize the much faster computation rather than the nonlinear schemes with the same level of accuracy. In this paper, numerical experiments are carried out to demonstrate efficiency of the proposed scheme.

Key words. Stefan problem, Porous medium equation, Cross-diffusion system, Degenerate convection-reaction-diffusion equation, Linear scheme, Error estimate, Numerical method

AMS subject classifications. 35K55, 65M12, 80A22, 92D25

1. Introduction. In this paper, we propose an efficient linear scheme for the following nonlinear diffusion problem: Find $\boldsymbol{z} = (z_1, \dots, z_M) : \overline{\Omega} \times [0, T) \to \mathbb{R}^M$ $(M \in \mathbb{N})$ such that

$$\begin{cases} \dfrac{\partial \boldsymbol{z}}{\partial t} = \Delta \boldsymbol{\beta}(\boldsymbol{z}) + \boldsymbol{f}(\boldsymbol{z}) & \text{in} \quad Q := \Omega \times (0,T), \\ \boldsymbol{\beta}(\boldsymbol{z}) = \boldsymbol{0} & \text{on} \quad \partial\Omega \times (0,T), \\ \boldsymbol{z}(\cdot, 0) = \boldsymbol{z}^0 & \text{in} \quad \Omega. \end{cases} \tag{1.1}$$

Here, $\Omega \subset \mathbb{R}^d$ $(d \in \mathbb{N})$ is a bounded domain with smooth boundary $\partial\Omega$, T is a positive constant, $\boldsymbol{\beta} = (\beta_1, \dots, \beta_M)$, $\boldsymbol{f} = (f_1, \dots, f_M)$: $\mathbb{R}^M \to \mathbb{R}^M$ and $\boldsymbol{z}^0 = (z_1^0, \dots, z_M^0) \in L^2(\Omega)^M$ are given functions. Let $(\beta_i)_j$ denote the derivative of the ith component of $\boldsymbol{\beta}$ with respect to the jth variable. If there is a point s where $(\beta_i)_i(s) = 0$ for some i, then the diffusion vanishes at that point. In this case, (1.1) is called a degenerate parabolic system. This type of problem with $M = 1$ includes the Stefan problem and the porous medium equation, and such problems have been widely studied for a long time. In Problem (1.1), the diffusivity β_i of the ith component depends not only on the ith variable but also on the jth $(j \neq i)$ variables in general. This mixture of diffusion terms is called cross-diffusion. This type of problems appears in many fields of applications. A typical example is called the Shigesada-Kawasaki-Teramoto cross-diffusion system [9].

In this paper, we propose an efficient numerical scheme to approximate the solutions of Problem (1.1). Our scheme has many advantages, e.g., it is very easy-to-implement and stable, computational costs are low, the discretization matrices are symmetric, and the accuracy is comparable to that of the widely studied nonlinear

*Department of Mathematics and Computer Science, National University of Lesotho, P.O. Roma 180, Lesotho (m.molati@nul.ls).
†Faculty of Mathematics, Kyushu University, 744 Motooka, Nishiku, Fukuoka 819-0395, Japan(murakawa@math.kyushu-u.ac.jp) (Corresponding author).

schemes. The contents of this paper are as follows. In the next section, we give a brief introduction of numerical schemes for (1.1) which are covered in the literature. In Section 3, we propose an efficient linear scheme, and give a brief summary of theoretical results. In Section 4, the numerical experiments are carried out. The numerical results illustrate the efficiency of the proposed scheme. Concluding remarks are made in the final section of the paper.

2. Numerical schemes. Before proposing our scheme, let us summarize numerical schemes in the literature (see references in [8]). We discuss discrete-time approximations. They are simpler than fully discrete numerical schemes but play a crucial role in developing numerical methods. Put $\tau = T/N_T$ ($N_T \in \mathbb{N}$) be the time step size. Let $\boldsymbol{Z}^0$ and $\boldsymbol{Z}^n (n = 1, \ldots, N_T)$denote the approximations of the initial function $\boldsymbol{z}^0$ and the solution $\boldsymbol{z}(\cdot, \tau n)$ at time $t = \tau n$, respectively. When we consider the 'equation' (1.1), that is, the case where $M = 1$, we do not use boldfaced variables and omit the subscript for the component. A lot of numerical schemes have been developed and analyzed for equation (1.1). Many researchers have considered nonlinear schemes of the following type:

$$\begin{cases} \dfrac{\beta_\varepsilon^{-1}(U^n) - \beta_\varepsilon^{-1}(U^{n-1})}{\tau} = \Delta U^n + f(\beta_\varepsilon^{-1}(U^n)) & \text{in} \quad \Omega, \\ U^n = 0 & \text{on} \quad \partial\Omega, \\ Z^n := \beta_\varepsilon^{-1}(U^n) & \text{in} \quad \Omega. \end{cases} \tag{2.1}$$

Here, the auxiliary functions U^n represent approximations to $\beta(z(\cdot, \tau n))$, and β_ε is a smooth and strictly increasing function which regularizes the non-smooth and non-strictly increasing function β. Nonlinear schemes of type (2.1) show better accuracy in practice. For solving the corresponding nonlinear algebraic systems arising from fully implicit schemes, some iterative methods such as the Newton method have to be used to linearize the schemes. Therefore, it requires much time for numerical computation. Incidentally, nonlinear schemes of type (2.3) stated below are also employed for the degenerate parabolic equations. However, the algebraic systems arising in (2.3) are non-symmetric, while those in (2.1) are symmetric. Thus, schemes of type (2.1) are more convenient to handle than those of type (2.3), especially, in multi-dimensional case.

Berger, Brezis and Rogers [2] proposed the following linear scheme for the degenerate parabolic equation:

$$\begin{cases} \mu U^n - \tau \Delta U^n = \mu\beta(Z^{n-1}) + \tau f(Z^{n-1}) & \text{in} \quad \Omega, \\ U^n = 0 & \text{on} \quad \partial\Omega, \\ Z^n := Z^{n-1} + \mu(U^n - \beta(Z^{n-1})) & \text{in} \quad \Omega. \end{cases} \tag{2.2}$$

Here, μ is a given positive constant. This is quite simple in that the scheme amounts to solving linear elliptic equations in U^n and then to performing explicit corrections for Z^n. After discretizing this scheme in space, we obtain an easy-to-implement numerical method. Implementation and calculation time are almost the same as the implicit method for the linear heat equation requires. However, the accuracy is low compared with the nonlinear scheme because the nonlinear diffusion is approximated by the linear diffusion with a constant diffusion coefficient.

The history of numerical analysis for the cross-diffusion systems is not long, and the list of references is very short compared to the one for the degenerate parabolic

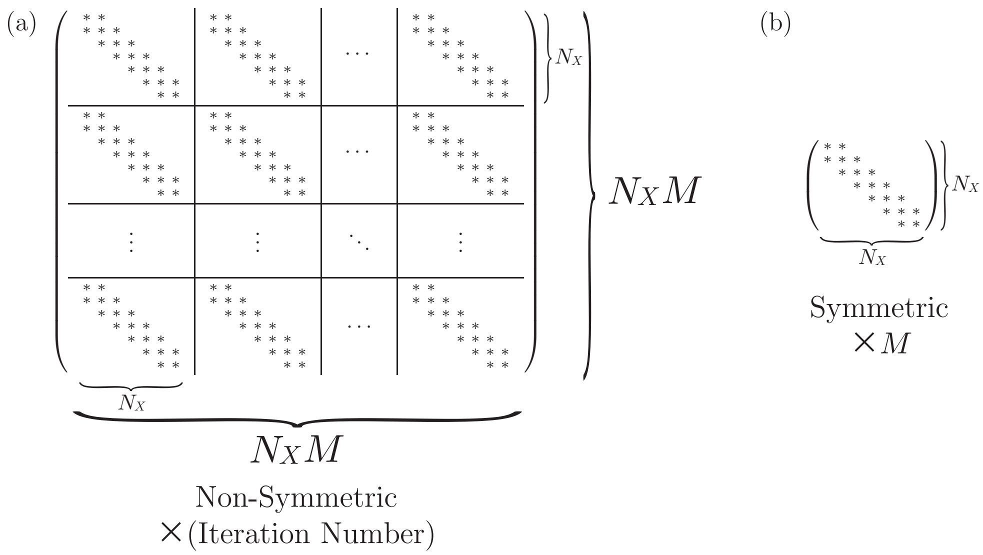

FIG. 2.1. (a) *Type of matrices arising in the nonlinear scheme* (2.3) *in one space dimension.* (b) *Type of matrices arising in the linear schemes* (2.4) *and* (3.1) *in one space dimension. Here,* N_X *and* M *denote the numbers of spatial mesh points and components in* (1.1), *respectively.*

equations. Most researchers have treated the following type of fully implicit nonlinear schemes.

$$\begin{cases} \dfrac{\boldsymbol{Z}^n - \boldsymbol{Z}^{n-1}}{\tau} = \Delta\boldsymbol{\beta}(\boldsymbol{Z}^n) + \boldsymbol{f}(\boldsymbol{Z}^n) & \text{in} \quad \Omega, \\ \boldsymbol{\beta}(\boldsymbol{Z}^n) = \boldsymbol{0} & \text{on} \quad \partial\Omega. \end{cases} \tag{2.3}$$

The matrices generated by the discretization in space are large, sparse and non-symmetric even in one space dimension (FIG 2.1(a)). The implementation is complicated and the computational costs are high. In multi-component case and/or in multi-dimensional space, this drawback becomes even bigger.

In references [5, 6, 7], the author proposed and analyzed the following linear scheme for the cross-diffusion system (1.1):

$$\begin{cases} \mu\boldsymbol{U}^n - \tau\Delta\boldsymbol{U}^n = \mu\boldsymbol{\beta}(\boldsymbol{Z}^{n-1}) + \tau\boldsymbol{f}(\boldsymbol{Z}^{n-1}) & \text{in} \quad \Omega, \\ \boldsymbol{U}^n = \boldsymbol{0} & \text{on} \quad \partial\Omega, \\ \boldsymbol{Z}^n := \boldsymbol{Z}^{n-1} + \mu(\boldsymbol{U}^n - \boldsymbol{\beta}(\boldsymbol{Z}^{n-1})) & \text{in} \quad \Omega. \end{cases} \tag{2.4}$$

This scheme is regarded as an extension of (2.2) to the system. Likewise, the scheme amounts to solving M independent linear elliptic equations in $\boldsymbol{U}^n$ and updating $\boldsymbol{Z}^n$ explicitly. The boundary condition becomes quite simple. The difficulty of implementation is almost the same as appears in the implicit method for the linear heat equation. The computational cost is less than M times the computational cost of the linear heat equation, because the ensuing linear algebraic system keeps the same matrix for all time steps and for all $i \in \{1, \dots, M\}$. The type of matrices is shown in FIG 2.1(b).

3. Proposed linear scheme. Taking the advantages and disadvantages of the nonlinear and the linear schemes into consideration, we modify the linear scheme

(2.4), and then, propose an efficient linear scheme for Problem (1.1).

We rewrite equation (1.1) with $M = 1$ and the linear scheme (2.2) formally as follows:

$$\begin{cases} \dfrac{1}{\beta'(z)}\dfrac{\partial\beta(z)}{\partial t} = \Delta\beta(z) + f(z), \\ \dfrac{\partial z}{\partial t} = \dfrac{1}{\beta'(z)}\dfrac{\partial\beta(z)}{\partial t}, \end{cases} \qquad \begin{cases} \mu\dfrac{U^n - \beta(Z^{n-1})}{\tau} = \Delta U^n + f(Z^{n-1}), \\ \dfrac{Z^n - Z^{n-1}}{\tau} = \mu\dfrac{U^n - \beta(Z^{n-1})}{\tau}. \end{cases}$$

By comparing these expressions, the parameter μ can be regarded as an approximation to $1/\beta'(z)$. In practice, we usually choose $\mu = L_\beta^{-1}$, where L_β is the Lipschitz constant of β. But the accuracy of the numerical solutions is low, because of the rough choice of μ. So, it is expected that a good approximation μ to $1/\beta'(z)$ gives the numerical solution with high accuracy, for example, $\mu \approx 1/\beta'(Z^{n-1})$. Along this idea, Murakawa [8] proposed the following scheme for Problem (1.1).

$$\begin{cases} \mu_i^n U_i^n - \tau\Delta U_i^n = \mu_i^n \beta_i(\boldsymbol{Z}^{n-1}) + \tau f_i(\boldsymbol{Z}^{n-1}) & \text{in} \quad \Omega, \\ U_i^n = 0 & \text{on} \quad \partial\Omega, \\ Z_i^n = Z_i^{n-1} + \mu_i^n(U_i^n - \beta_i(\boldsymbol{Z}^{n-1})) & \text{in} \quad \Omega \end{cases} \quad (i = 1, \ldots, M). \tag{3.1}$$

Here, $\mu_i^n = \mu_i^n(x)$ $(i = 1, \ldots, M)$ are given functions. Thus, we just change μ from a constant to functions. This minor change makes the scheme more accurate. The difficulty of implementation and computational costs do not greatly differ from those of (2.2) and (2.4).

The shape of matrices arising in the scheme (3.1) is the same as in the implicit scheme for the linear heat equation (FIG 2.1(b)). Since the matrices are symmetric, we can employ efficient solver such as conjugate gradient method. On the other hand, the matrices arising in the scheme (2.3) (FIG 2.1(a)) are large, sparse and non-symmetric even in one space dimension. Moreover, computational costs are high.

Rates of convergence of (3.1) with respect to τ were derived theoretically in [8]. Since there is some difference between the handling of the degenerate-diffusion and that of the cross-diffusion from mathematical points of view, it is difficult to treat degenerate cross-diffusion systems in general settings. Therefore, we deal with each case separately. The results can be summarized as follows. Let $\boldsymbol{z}$ be the weak solution of (1.1), and $\boldsymbol{U}$, $\boldsymbol{Z}$ be piecewise constant interpolations in time of a solution of (3.1). We define the global error E by

$$\begin{aligned} E := & \|\boldsymbol{\beta}(\boldsymbol{z}) - \boldsymbol{U}\|_{L^2(Q)^M} + \left\| \int_0^t (\boldsymbol{\beta}(\boldsymbol{z}) - \boldsymbol{U}) \right\|_{L^\infty(0,T;H^1(\Omega))^M} \\ & + \|\boldsymbol{z} - \boldsymbol{Z}\|_{L^\infty(0,T;H^{-1}(\Omega))^M}. \end{aligned}$$

Then, the following orders were derived under some assumptions.

- For degenerate parabolic systems (without cross-diffusion),

$$\boldsymbol{z}^0 \in L^2(\Omega)^M \implies E = O(\tau^{1/4}), \tag{3.2}$$

$$\boldsymbol{z}^0 \in L^\infty(\Omega)^M,\ \Delta\boldsymbol{\beta}(\boldsymbol{z}^0) \in L^1(\Omega)^M \implies E = O(\tau^{1/2}). \tag{3.3}$$

- For (non-degenerate) cross-diffusion systems,

$$\boldsymbol{z}^0 \in L^2(\Omega)^M \implies E + \|\boldsymbol{z} - \boldsymbol{Z}\|_{L^2(Q)^M} = O(\tau^{1/2}), \tag{3.4}$$

$$\boldsymbol{z}^0 \in H_0^1(\Omega)^M \implies E + \|\boldsymbol{z} - \boldsymbol{Z}\|_{L^2(Q)^M} = O(\tau). \tag{3.5}$$

The orders (3.3)–(3.5) are sharp on account of the global regularity in time. These optimal error estimates (3.2)–(3.5) are the same as in the case where μ is a constant, and were obtained by Magenes, Nochetto and Verdi [3] for the degenerate parabolic equations and by Murakawa [6] for the cross-diffusion systems. However, actual errors in numerical computation become significantly smaller if we choose $\mu_i^n(x)$ suitably.

4. Numerical experiments. In this section, we carry out numerical experiments in one space dimension in order to demonstrate the performance of our scheme. Both the nonlinear and the linear schemes are tried, and these schemes are discretized in space by the standard finite difference method with a uniform mesh. All experiments were performed on a Laptop equipped with Intel Core(TM) i7-3667U CPU using a single thread. The C sources are complied by the GCC compiler with option -O3.

We calculate the discrete relative $L^2(Q)^M$ error $E_{\beta(z)}$, namely,

$$E_{\beta(z)} = \left(\sum_{\substack{0\le j\le N_X \\ 1\le n\le N_T}} \left| \boldsymbol{U}^{j,n} - \boldsymbol{\beta}(\boldsymbol{z}(x_j, n\tau)) \right|^2 \Big/ \sum_{\substack{0\le j\le N_X \\ 1\le n\le N_T}} \left| \boldsymbol{\beta}(\boldsymbol{z}(x_j, n\tau)) \right|^2 \right)^{1/2}.$$

Here, $N_X + 1$ is the number of mesh points and x_j $(0 \le j \le N_X)$ imply the spatial grid points.

4.1. The porous medium equation. We deal with the following porous medium equation, that describes the isentropic flow through a porous medium.

$$\frac{\partial z}{\partial t} = \Delta z^m \quad \text{in } \Omega \times (0, T], \tag{4.1}$$

where $m > 1$, $\Omega = (-L, L) = (-8, 8)$ and $T = 10$. With appropriately chosen initial and boundary data, this problem has the following exact solution, which was derived by Barenblatt [1]:

$$z(x,t) = \frac{1}{(t+1)^{m+1}} \left[1 - \frac{(m-1)x^2}{2m(m+1)(t+1)^{\frac{2}{m+1}}} \right]_+^{\frac{1}{m-1}}.$$

Here, $[\cdot]_+$ implies the positive part. For the nonlinear scheme, the following approximate inverse function with $\varepsilon = 10^{-4}$ is used:

$$\beta_\varepsilon^{-1}(u) = \begin{cases} u^{\frac{1}{m}} & \text{if } u \ge \varepsilon^{\frac{m}{m-1}}, \\ \dfrac{1}{\varepsilon} u & \text{otherwise.} \end{cases}$$

For the linear schemes, we set $\mu = 1/m$ in the fixed μ case, and choose μ^n as follows in the case where μ^n are functions:

$$\mu^n = 1/(10^{-3} + \beta'(Z^{n-1})).$$

The spatial mesh size is fixed as $h = 2L/N_X = 2^{-10}$ and we inquire into rates of convergence with respect to the time step size τ. We consider the case where $m = 16$. The Barenblatt solution is shown in FIG 4.1(a). FIG 4.1(b) illustrates errors versus time step size with $\tau = 2^{-4}, 2^{-5}, \ldots, 2^{-9}$. The errors in the proposed linear

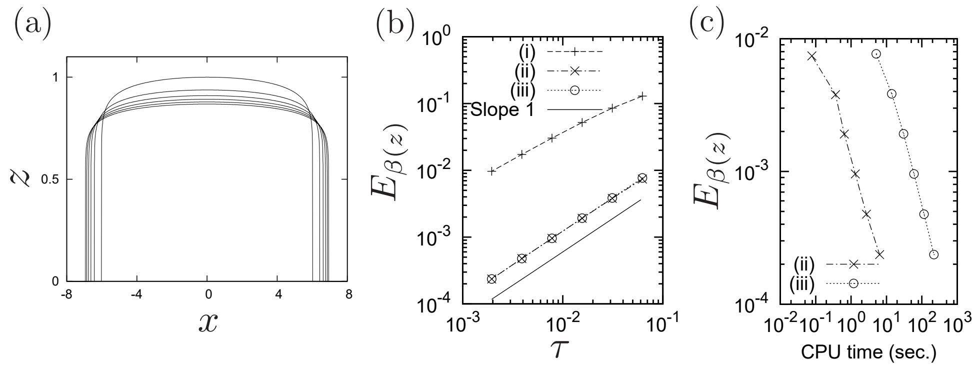

FIG. 4.1. (a) *The Barenblatt solution of the porous medium equation* (4.1) *with* $m = 16$ *at* $t = 0, 2, \ldots, 10$. (b), (c) *Numerical results for the porous medium equation* (4.1), *where* (i) *represents the linear scheme* (2.2), (ii) *represents the linear scheme* (3.1), (iii) *represents the nonlinear scheme* (2.1).

scheme (3.1) and in the nonlinear scheme (2.1) are almost the same, and are quite smaller than those in the linear scheme (2.2) with fixed μ. The errors are along a straight line having slope 1, which implies that the numerical rate of convergence with respect to τ is of order 1 for each scheme. This is much better than the theoretical result (3.3). The proposed linear and the nonlinear schemes are compared in terms of CPU time. The results are shown in FIG 4.1(c). The proposed linear scheme is about 50 times faster than the nonlinear scheme to achieve the same level of accuracy in this experiment. These results indicate that the proposed linear scheme is superior in speed to the nonlinear scheme even though the linear scheme is very easy-to-implement and it is computationally less costly. These advantages become even more when we deal with higher dimensional and/or multi-component problems.

4.2. The Shigesada-Kawasaki-Teramoto cross-diffusion system. We deal with the following cross-diffusion system that was proposed by Shigesada, Kawasaki and Teramoto [9] to understand temporal and spatial behaviours of two animal species under the influence of the population pressure due to intra- and interspecific interferences:

$$\begin{cases} \dfrac{\partial z_1}{\partial t} = \Delta\left[(a_{10} + a_{11} z_1 + a_{12} z_2) z_1\right] + (c_{10} - c_{11} z_1 - c_{12} z_2) z_1 + f_1(x,t), \\ \dfrac{\partial z_2}{\partial t} = \Delta\left[(a_{20} + a_{21} z_1 + a_{22} z_2) z_2\right] + (c_{20} - c_{21} z_1 - c_{22} z_2) z_2 + f_2(x,t). \end{cases} \tag{4.2}$$

Here, we set $a_{10} = 1$, $a_{20} = 1/(3c_{12})$, $c_{10} = 1$, $c_{11} = 1$, $c_{12} = 2.5$, $c_{20} = 1$,

$c_{21} = 2 + 5c_{20}/3 - c_{20}c_{12}$, $c_{22} = 1$, and

$$\begin{aligned}
f_1(x,t) =& \frac{1}{32}\mathrm{sech}\left(\frac{1}{4}(t+\sqrt{2}x)\right)^4 \Bigg(-4a_{11} + 2a_{12} + (2a_{11} - 5a_{12})\tanh\left(\frac{1}{4}(t+\sqrt{2}x)\right) \\
&+ \cosh\left(\frac{1}{2}(t+\sqrt{2}x)\right)\left(2a_{11} - a_{12} + (2a_{11}+a_{12})\tanh\left(\frac{1}{4}(t+\sqrt{2}x)\right)\right)\Bigg), \\
f_2(x,t) =& \frac{1}{64}\mathrm{sech}\left(\frac{1}{4}(t+\sqrt{2}x)\right)^4 \left(-1 + \tanh\left(\frac{1}{4}(t+\sqrt{2}x)\right)\right) \\
&\times \Bigg(-7a_{21} + 10a_{22} + 3(a_{21} - 2a_{22})\tanh\left(\frac{1}{4}(t+\sqrt{2}x)\right) \\
&+ \cosh\left(\frac{1}{2}(t+\sqrt{2}x)\right)\left(5a_{21} - 4a_{22} + (3a_{21}+4a_{22})\tanh\left(\frac{1}{4}(t+\sqrt{2}x)\right)\right)\Bigg).
\end{aligned}$$

This problem has the following exact solution:

$$\begin{aligned}
z_1(x,t) &= \frac{1}{2}\left(1 + \tanh\left(\frac{1}{4}(t+\sqrt{2}x)\right)\right), \\
z_2(x,t) &= \frac{1}{4}\left(1 - \tanh\left(\frac{1}{4}(t+\sqrt{2}x)\right)\right)^2.
\end{aligned} \tag{4.3}$$

The functions f_1 and f_2 are determined so that (z_1, z_2) defined in (4.3) is a solution of system (4.2).

We carry out numerical experiments with $a_{11} = 0$, $a_{12} = 10$, $a_{21} = 10$, $a_{22} = 0$ in space $\Omega = (0, 10)$ and in time interval $(-10, -5)$. The spatial mesh size is fixed as $h = 2^{-8}$. The initial and the Dirichlet boundary data are given by the exact solution. The solution is shown in FIG 4.2(a). Looking at the shapes of matrices arising in the

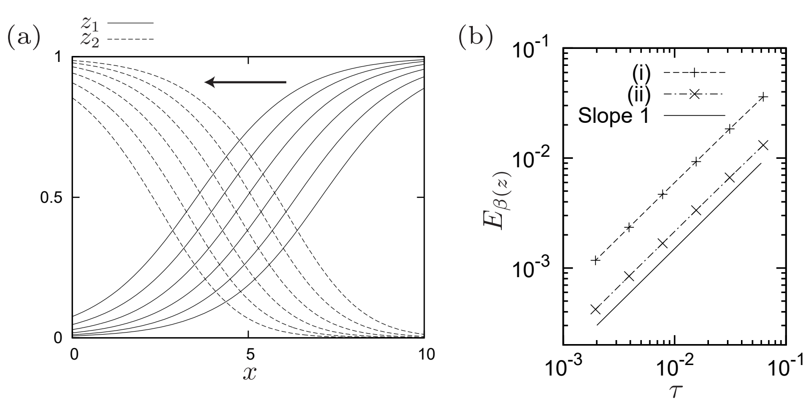

FIG. 4.2. (a) *The solution of* (4.2) *at* $t = -10, -9, \ldots, -5$. (b) *Numerical results for* (4.2), *where* (i) *and* (ii) *represent the linear schemes* (2.4) *and* (3.1), *respectively.*

schemes, which are shown in FIG 2.1, it is easy to imagine that the linear scheme (3.1) is superior than the nonlinear scheme (2.3) in terms of simplicity of implementation and computational costs. We treat only the linear schemes (2.4) and (3.1) in the case where μ is fixed as $\mu = 0.1$ and in the case where μ_i^n are functions, respectively. Using $\boldsymbol{Z}^{n-1}$, we define μ_i^n as follows:

$$\mu_i^n(x) = 1/(\beta_i)_i(\boldsymbol{Z}^{n-1}(x)).$$

In the fixed μ case, if we choose μ_i larger than 0.1, then the numerical solutions become unstable. FIG 4.2(b) shows the numerical results with $\tau = 2^{-4}, 2^{-5}, \ldots, 2^{-9}$. Numerical convergence rate with respect to τ is observed to be of order 1, which corresponds to the theoretical result. The proposed scheme (3.1) shows higher accuracy compared to the fixed μ case. The difference (about three times difference) is not so large in this experiment. This difference becomes considerably large in the problem of which solution shows the profile with sharp peaks (see Section 5.4 in [8]).

4.3. A degenerate convection-reaction-diffusion equation. We deal with the following degenerate convection-reaction-diffusion equation in one space dimension:

$$\frac{\partial z}{\partial t} = \frac{\partial}{\partial x^2}\beta(z) - \frac{\partial}{\partial x}(b_1 z - b_2\beta(z)) - c(z - \beta(z)), \tag{4.4}$$

where $b_1, b_2, c \in \mathbb{R}$. The function β is defined as follows.

$$\beta(s) := [\![s]\!]^m := \begin{cases} s^m & \text{if } s \geq 0, \\ -(-s)^m & \text{if } s < 0. \end{cases}$$

This problem has the following exact solution [4].

$$z(x,t) = k_1 \exp\left(-ct - \frac{b_2(x - b_1 t)}{2m}\right)\left[\!\!\left[\cos\left(\frac{1}{2}(x - b_1 t - k_2)\sqrt{4c - b_2^2}\right)\right]\!\!\right]^{1/m},$$

where k_1 and k_2 are arbitrary constants. Since $\cos(\sqrt{-1}x) = \cosh x$, the value in the bracket on the right hand side can be determined for arbitrary parameters.

The linear scheme (3.1) can be applied to this problem because (4.4) is linear in z and $\beta(z)$. Therefore, we have the following linear scheme for (4.4).

$$\begin{cases} \mu^n \dfrac{U^n - \beta(Z^{n-1})}{\tau} = \dfrac{\partial}{\partial x^2}U^n - \dfrac{\partial}{\partial x}(b_1 Z^n - b_2 U^n) - c(Z^n - U^n), \\ Z^n = Z^{n-1} + \mu^n(U^n - \beta(Z^{n-1})). \end{cases}$$

Substituting the second equation into the first one, we have

$$\begin{cases} ((1+\tau c)\mu^n - \tau c)U^n - \tau\dfrac{\partial}{\partial x^2}U^n + \tau\dfrac{\partial}{\partial x}((b_1\mu^n - b_2)U^n) \\ \qquad = (1+\tau c)\mu^n\beta(Z^{n-1}) - \tau c Z^{n-1} - \tau b_1\dfrac{\partial}{\partial x}(Z^{n-1} - \mu^n\beta(Z^{n-1})), \\ Z^n = Z^{n-1} + \mu^n(U^n - \beta(Z^{n-1})). \end{cases} \tag{4.5}$$

This scheme, which consists of solving the linear problem in U^n and explicit correction for Z^n, is quite simpler than nonlinear schemes.

We carry out numerical simulations for (4.4). We set $m = 10$, $b_1 = 2mc/b_2$, $b_2 = c = k_2 = 1$, $k_1 = 3\pi/4$, $\Omega = (0, L) = (0, 10)$, $(0, T) = (0, 0.05)$. The exact solution is presented in FIG 4.3(a). Because of the appearance of the convection term, we set $\tau = h/(4L)$ and used the standard upwind technique. We deal with the linear schemes with fixed μ and with varying $\mu^n(x)$. These parameters are chosen to be the same as used in Subsection 4.1. FIG 4.3(b) shows the numerical results with $h = 2^{-6}, 2^{-7}, \ldots, 2^{-10}$, which demonstrates numerical convergence of both linear schemes. The numerical rates of convergence with respect to h (and/or τ) is slightly less than 1. The scheme with varying μ shows higher accuracy than the linear scheme with fixed μ.

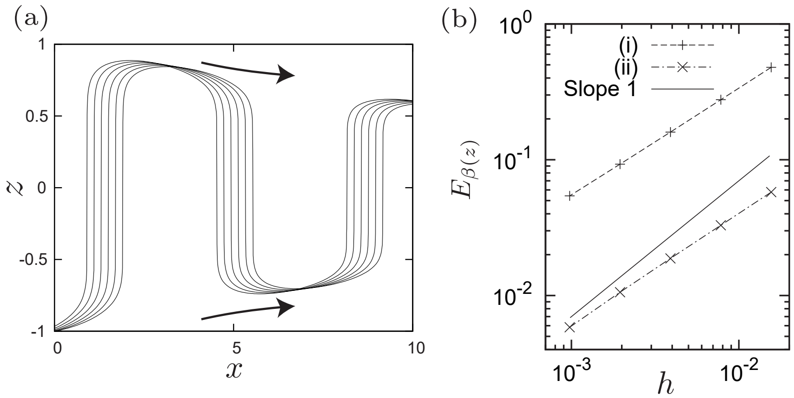

FIG. 4.3. (a) *The solution of* (4.4) *at* $t = 0, 0.01, \ldots, 0.05$. (b) *Numerical results for* (4.4), *where* (i) *represents the linear scheme* (4.5) *with fixed* μ, (ii) *represents the linear scheme* (4.5) *with varying* $\mu^n(x)$.

5. Conclusion. The linear scheme with simple implementation has been proposed instead of the widely used nonlinear schemes for the nonlinear diffusion problem (1.1). The motivation is based on the fact that the proposed linear scheme (3.1), which is an improvement of the linear scheme (2.4), retains the same accuracy as obtained from the nonlinear schemes (2.1) and (2.3) with less difficulty of the implementation. The difficulty is much the same as for the linear heat equation, whereas the advantages are many. For instance, the type of linear algebraic systems in (3.1) is the same as in the implicit method for the linear heat equation. Moreover, it is easy to set the parameters appropriately and the computational costs are low. These advantages and those mentioned earlier work as well even for multi-dimensional and multi-component systems. On the other hand, in general, the nonlinear schemes are complicated to implement and require high computational costs. Taking account of accuracy, efficiency, stability and computational cost into consideration, we proposed the linear scheme with simple implementation, of which advantages are proved in complicated problem such as (4.4).

Acknowledgments. This work was partially supported by JSPS KAKENHI Grant nos. 26287025, 15H03635 and 17K05368, and JST CREST Grant No. JPMJCR14D3. MM acknowledges the Matsumae International Foundation for financial support and the Faculty of Mathematics at Kyushu University for hosting him during the research fellowship.

REFERENCES

[1] G.I. BARENBLATT, *On some unsteady motion of a liquid or a gas in a porous medium*, Prikl. Math. Meh., 16 (1952), pp. 67–78.

[2] A.E. BERGER, H. BREZIS AND J.C.W. ROGERS, *A numerical method for solving the problem* $u_t - \Delta f(u) = 0$, R.A.I.R.O. Anal. Numér., 13 (1979), pp. 297–312.

[3] E. MAGENES, R.H. NOCHETTO AND C. VERDI, *Energy error estimates for a linear scheme to approximate nonlinear parabolic problems*, Math. Mod. Numer. Anal., 21 (1987), pp. 655–678.

[4] M. MOLATI AND H. MURAKAWA, *Exact solutions of nonlinear diffusion-convection-reaction equation: A Lie symmetry analysis approach*, preprint.

[5] H. Murakawa, *A linear scheme to approximate nonlinear cross-diffusion systems*, Math. Mod. Numer. Anal., 45 (2011), pp. 1141–1161.

[6] H. Murakawa, *Error estimates for discrete-time approximations of nonlinear cross-diffusion systems*, SIAM J. Numer. Anal., 52(2) (2014), pp. 955–974.

[7] H. Murakawa, *A linear finite volume method for nonlinear cross-diffusion systems*, Numer. Math., 136(1) (2017), pp. 1–26.

[8] H. Murakawa, *An efficient linear scheme to approximate nonlinear diffusion problems*, to appear in Jpn. J. Ind. Appl. Math., DOI: 10.1007/s13160-017-0279-3.

[9] N. Shigesada, K. Kawasaki and E. Teramoto, *Spatial segregation of interacting species*, J. Theor. Biol., 79 (1979), pp. 83–99.